Astronomy & Astrophysics manuscript no. output
December 3, 2019

The Orbital Surface Density Distribution and Multiplicity of M-Dwarfs

N. Susemiehl[1] and M. Meyer[1,]

Department of Astronomy, University of Michigan, Ann Arbor, MI, USA

2019

ABSTRACT

Aims. We present a new estimate of the multiplicity fraction of M-Dwarfs using a log-normal fit to the orbital surface density distribution.
Methods. We used archival data from five M-Dwarf multiplicity surveys to fit a log-normal model to the orbital surface density distribution of these stars. This model, alongside the companion mass ratio distribution given by Reggiani and Meyer (2013), was used to calculate the frequency of companions over the ranges of mass ratio (q) and semi-major axis (a) that the referenced surveys were collectively sensitive over - [0.60 ≤ q ≤ 1.00] and [0.00 ≤ a ≤ 10,000 AU]. This method was then extrapolated to calculate a multiplicity fraction which encompasses the broader ranges of [0.10 ≤ q ≤ 1.00] and [0.00 ≤ a < ∞ AU]. Finally, the results of these calculations were compared to the multiplicity fractions of other spectral types of stars.
Results. The multiplicity fraction over the constrained regions of [0.60 < q < 1.00] and [0.00 ≤ a ≤ 10,000 AU] was found to be 0.239 ± 0.040. The extrapolated multiplicity fraction over the broader ranges of q (0.10 - 1.00) and a (0.00 - ∞ AU) was calculated as 0.475 ± 0.129. Lastly, evidence was uncovered which suggests that the multiplicity of M-Dwarfs is similar to that of FGK and A stars over the constrained regions of mass ratio and semi-major axis.

Key words. binary stars – M-Dwarfs – stellar demographics

1. Introduction

1.1. Background

M-Dwarfs are among the most numerous stars in the universe, and many exist alongside at least one companion. Various attempts have been made to find the multiplicity fraction of M-Dwarfs (Fischer & Marcy 1992, Janson et. al. 2012, Winters 2019), but this value is not yet well constrained. Knowing this will have important implications for star formation theories, inform us about the emergence of planetary systems around low mass stars, and allow for the modeling of both galactic and extragalactic stellar populations.

Fundamentally, the multiplicity fraction of a population of stars depends on the companion mass ratio distribution (ψ) and the orbital surface density distribution (ϕ). The mass ratio, q, is defined as: $\frac{M_{secondary}}{M_{primary}}$ where, by definition, $M_{primary} > M_{secondary}$ so that $q \leq 1$. Furthermore, the semi-major axis, a, of a system serves as a measure of the separation between the primary and secondary stars. Using these two components, we calculate the multiplicity fraction as:

$$f = \int_{q_{min}}^{q_{max}} \psi dq * \int_{log_{10}a_{min}}^{log_{10}a_{max}} \phi dlog_{10}(a) \quad (1)$$

where $q_{min}, q_{max}, log_{10}a_{min}$, and $log_{10}a_{max}$ represent the lower and upper bounds for the regions of mass ratio and semi-major axis of interest. The first integral, the companion mass ratio distribution, is discussed in Reggiani & Meyer (2013). The authors of this paper find that the formula:

$$\psi = \frac{dN}{dq} = q^{.25\pm0.29} \quad (2)$$

describes this distribution for M-Dwarfs and other types of stars. This work has focused on finding the functional form for ϕ in Equation (1), the orbital surface density distribution. Once this is determined, Equation (1) can be used to calculate the multiplicity of M-Dwarfs by integrating over specific ranges of mass ratio and semi-major axis. This method for calculating the multiplicity fraction is built upon a key assumption: that the mass ratio distribution does not depend on orbital separation. Evidence for this is provided by Reggiani & Meyer (2013) and is further discussed in Section 4.4 of this work. Assuming this independence allows for the calculation of multiplicity as stated above. Furthermore, the method used in this paper for calculating multiplicity only takes into consideration binary systems and not triplets, quadruplets, etc. This is further discussed in Section 4.3.

2. Methods

2.1. Acquiring the Data

The first step in exploring the orbital surface density distribution and multiplicity of M-Dwarfs was to compile data from a variety of different multiplicity surveys in order to build the model. Data was taken from surveys which employed the radial velocity (Delfosse et. al. (1998), Fischer and Marcy (1992)) and direct imaging (Cortes-Contreras et. al. (2016), Janson et. al. (2012), and Ward Duong et. al. (2015)) companion detection methods. These would later be used as point estimates of the multiplicity fraction for the purposes of fitting a model to the orbital surface density distribution. Incorporating data which arose from these two different detection methods allowed us to investigate companions with broad ranges of semi-major axes. Additional

surveys utilizing microlensing or astrometry detection methods were not used in this analysis because the radial velocity and direct imaging surveys listed above were found to adequately represent the full range of semi-major axis.

In order to ensure the certainty of companion detections made by each referenced survey, we sought to constrain our analysis to only include detected multiple systems with the values of mass ratio and semi-major axis to which each survey was at least 90% complete. The limiting mass ratio, defined as the highest value of mass ratio that any of the five surveys was minimally sensitive to, was set by Cortes-Contreras et. al (2016) to be 0.60. Each of the other surveys were minimally sensitive to lower values of mass ratio, so the range of mass ratio that the referenced surveys are collectively sensitive to is therefore 0.60 - 1.00. For each survey, any detected multiple system which did not have a mass ratio between 0.60 and 1.00 and a separation within the range which that specific survey was 90% complete to was removed from our analysis entirely. This removal was done by striking any outlying multiple systems from the data and calculating a multiplicity fraction using the original total population number for each referenced survey. Table (1) depicts the point estimate of the multiplicity fraction for each survey along with the respective detection method and sensitive range of semi-major axis.

Making these cuts required a firm understanding of the ranges of mass ratio and semi-major axis that each of the five surveys were sensitive. In the case of some of the surveys, these ranges were not explicitly stated in the text and assumptions had to be made. Delfosse et. al. (1998) reported the period and orbital velocity of stars in their sample, but not the semi-major axis. To remedy this, Kepler's Third Law was used to convert the given values into a semi-major axis. Janson et. al. (2012) did not note the minimum mass ratio that the survey could detect. The authors state: "In every case where $q_m m_a < 0.08\ M_{sun}$, the system is removed from the analysis... Furthermore, we include only stars with primary mass $> 0.2\ M_{sun}$, since lower mass stars are not fully complete out to 52 pc." From this, we took a minimum secondary mass of $0.08\ M_{sun}$ and a minimum primary mass of $0.2\ M_{sun}$ and divided these to reach a limiting mass ratio of 0.4.

In certain cases, assumptions had to be made about other details of the surveys. Both Janson et. al. (2012) and Ward-Duong et. al. (2015) included a small number of multiple systems with K-type primary stars. Each system with a K-type primary was removed from this analysis, and the total sample number was reduced to only include M-dwarf primaries (both surveys state the number of K-type primaries sampled; this value was subtracted from the total number of stars sampled to arrive at a total number of M-dwarfs sampled). Because it covers such a wide range of semi-major axis (3 - 10,000 AU), the data from Ward-Duong et. al. (2015) was split into two bins by orbital separation: 0 - 100 AU and 100 - 10,000 AU. Conducting this split required the assumption that the two populations are independent. This is justified by the fact that the survey utilized two different companion confirmation methods for these two orbital separation regimes (archival plate analysis and adaptive optics imaging for the near and far separations respectively).

2.2. Fitting the Model

Next, we sought to fit a log-normal model to the orbital surface density distribution of the M-Dwarf multiple systems. This model, which we call ϕ, is described by:

$$\phi = \frac{dN}{dlog_{10}(a)} = A * \frac{e^{-(log_{10}(a)-log_{10}(\mu))^2/(2log_{10}(\sigma)^2)}}{log_{10}(\sigma) * \sqrt{2\pi}} \quad (3)$$

and has three free parameters: the amplitude (A), the base-10 log of mean ($log_{10}(\mu)$), and the base-10 log of standard deviation ($log_{10}(\sigma)$). In order to fit the model and find the best values for these parameters, a Markov Chain Monte Carlo (MCMC) routine was utilized. Model frequencies with the test parameters as input were compared to the frequencies from the data using a chi-squared log-likelihood function. Uniform log-priors were chosen with bound $0.0 \leq A \leq 2.0$, $-1.0 \leq log_{10}\mu \leq 2.0$, and $-1.0 \leq log_{10}\sigma \leq 2.0$. The MCMC was initialized with 100 walkers positioned randomly within the bound of the log-prior and ran for 5,000 steps. After this, the flattened chains of each of the three parameters were plotted in order to visualize the convergence of the walkers. This informed the decision to discard the first 200 steps of each flatchain as the burn-in values. The best fit amplitude, mean, and standard deviation were then calculated as the mean value of these chains, with error corresponding to the standard deviation of the respective flatchains. A cornerplot was produced which shows the distributions of each of the three parameters, and is shown below.

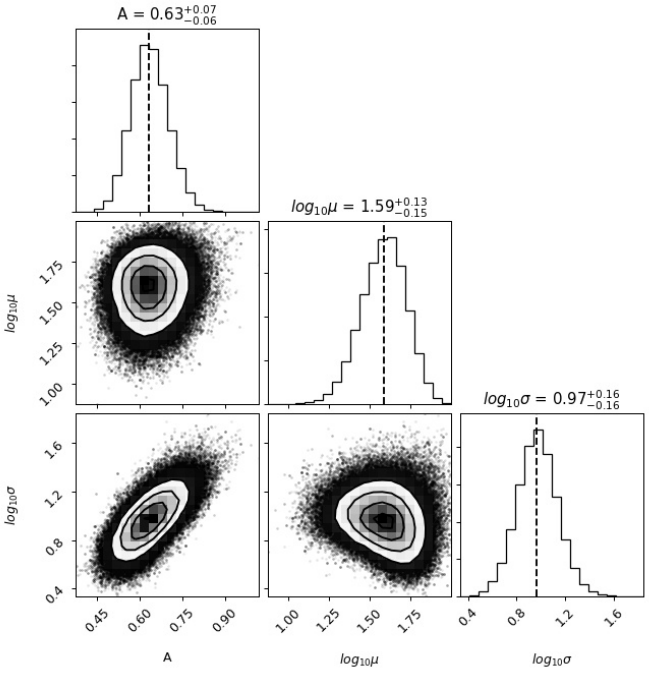

Fig. 1. This cornerplot shows the best fit values with error and marginal distributions of each of the three parameters as well as the covariances between all of them.

2.3. Calculating the Frequency

Next, the model for the orbital surface density distribution was used alongside the companion mass ratio distribution model from Reggiani and Meyer (2013) to calculate the multiplicity of M-Dwarfs as:

$$f = \int_{q_{min}}^{q_{max}} q^{.25} dq * A * \int_{log_{10}a_{min}}^{log_{10}a_{max}} \frac{e^{-(log_{10}(a)-log_{10}(\mu))^2/(2log_{10}(\sigma)^2)}}{log_{10}(\sigma) * \sqrt{2\pi}} dlog_{10}(a)$$

Table (1): Point Estimates of Multiplicity Fraction, q > 0.6

Reference	Detection Method	Semi-Major Axis Range (AU)	Multiplicity Estimate
Delfosse et. al. (1998)	RV	0.00 - 4.63	0.04 ± 0.018
Fischer & Marcy (1992)	RV	0.04 - 4.00	0.08 ± 0.034
Cortes-Contreras et. al. (2016)	DI	2.60 - 29.5	0.07 ± 0.012
Janson et. al. (2012)	DI	3.00 - 227.	0.18 ± 0.016
Ward-Duong et. al. (2015) A	DI	3.00 - 100.	0.11 ± 0.022
Ward-Duong et. al. (2015) B	DI	100. - 10,000.	0.07 ± 0.017

Table 1. This table depicts each of the M-Dwarf surveys used in this study alongside their respective detection method (RV for radial velocity and DI for direct imaging), the range of semi-major axis which the survey was at least 90% complete, and the point estimate of the multiplicity that we made after excluding companion detections outside the respective semi-major axis range and with q < 0.6.

(4)

This formula was first integrated over the ranges of q and a that encompass the survey data: $0.6 \leq q \leq 1.0$ and $0.00 \leq a \leq 10{,}000$ AU. This calculation resulted in a multiplicity fraction that is representative over these limited ranges of mass ratio and semi-major axis. These ranges were later expanded to $[0.10 \leq q \leq 1.0]$ and $[0 \leq a < \infty$ AU$]$ to allow for the calculation of a broader M-Dwarf multiplicity fraction. The error on the multiplicity fraction was calculated as the 90% confidence interval of the probability distribution function of the multiplicity fraction.

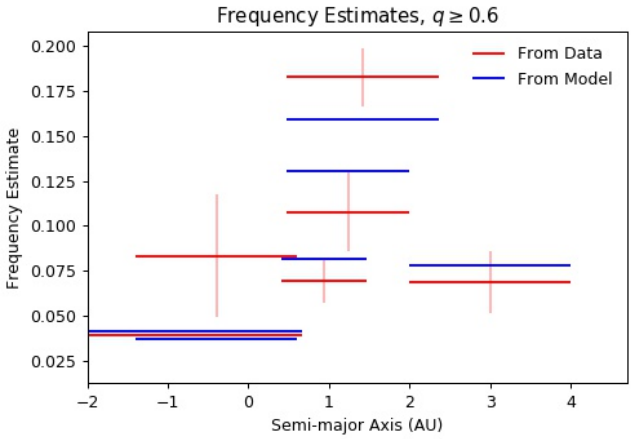

Fig. 2. This figure summarizes the multiplicity estimates from the source data and from the model. Each horizontal line has a y value of the frequency it represents and a width covering the range of semi-major axis it is representative over. The frequency values of the red lines, which come from the data, are also shown in Table (1). Each red line has a vertical error bar, representing the error in the frequency, which is also given in Table (1). The frequency value of each blue line is found by calculating the multiplicity using Equation (4) over the ranges of semi-major axis that each of the data points are representative over. Some of the frequencies calculated from the model do not fall in error of the frequencies from the data, as would be expected. This is discussed below.

3. Results

3.1. Orbital Surface Density Model

The best-fit to point estimates of frequency from the five M-Dwarf surveys resulted in the parameters of A, $log_{10}(\mu)$, and $log_{10}(\sigma)$, being 0.63 ± 0.065, 1.59 ± 0.140, and 0.97 ± 0.16 respectively. This fit is associated with a reduced chi-squared parameter value of 2.143. With three degrees of freedom, the chi-squared probability distribution indicates that the probability of achieving a value greater than or equal to 2.143 is 0.092. Despite this low probability, we fail to reject the null hypothesis that the data came from this model because it exceeds the 0.05 significance level. This indicates that the model is a weak fit to the data but can still be used to understand the distribution function. The log normal model with these best-fit parameter values of A, $log_{10}(\mu)$, and $log_{10}(\sigma)$, best describes the orbital surface density distribution of M-Dwarfs, assuming that this distribution is in fact log-normal in the semi-major axis.

3.2. Multiplicity Fraction

Integrating Equation (4) over the constrained regions of $[0.60 \leq q \leq 1.00]$ and $[0 \leq a \leq 10{,}000$ AU$]$ resulted in a multiplicity fraction of 0.236 ± 0.061. Following this process, a broad multiplicity fraction was found by integrating Equation (4) over $[0.1 \leq q \leq 1.0]$ and $[0.0 \leq a < \infty$ AU$]$ to be 0.475 ± 0.129. This broad multiplicity fraction considers stellar and sub-stellar companions to M-Dwarfs, but not planetary companions.

4. Discussion

4.1. The Multiplicity of M-Dwarfs

The results of this work and the multiplicity fraction calculated using the broad ranges of q and a suggest that around half of all M-Dwarfs have a companion. Because this estimate encompasses very small mass ratios, many of these companions may be Brown Dwarfs.

We sought to compare our model to the to the prediction of Bowler et. al. (2015), which estimated the frequency of Brown Dwarf companions to M-Dwarf hosts (which translates in this work to a low values of mass ratio). They predict the frequency of Brown Dwarf companions to M-Dwarf primaries over a semi-major axis range of 10 - 100 AU and mass ratio range of 0.039 - 0.224 to be $0.028^{+0.024}_{-0.015}$. We integrated Equation (1) with the best fit parameters described above over these ranges of semi-major axis and mass ratio and obtained an multiplicity estimate of 0.0277 ± 0.0093, which is within error of the result from Bowler. The proximity of our results with those of Bowler et. al. (2015) helps enforce the validity of our model.

4.2. Comparisons to Other Spectral Type Multiplicities

We also sought to compare the multiplicity of M-Dwarfs to that of the sun-like FGK- and more massive A-type stars over the constrained range of mass ratio and semi-major axis ($0.6 \leq q \leq 1.0$ and $0.00 \leq a \leq 10{,}000$ AU). To compare to the FGK multiplicity, we extrapolated the model of orbital surface density from Raghavan et. al. (2010) to integrate over the above range

of semi-major axis. This, alongside the companion mass ratio distribution from Reggiani Meyer (2013) described in Equation (2) and the full multiplicity equation, Equation (1), was used to find an FGK star multiplicity fraction of 0.230 ± 0.032, where the error is estimated as the Poisson counting error based on the survey of Raghavan et. al. (2010). We used the same method for the A star multiplicity fraction, this time referencing De Rosa et. al. (2013), and found a multiplicity fraction of 0.238 ± 0.026.

4.3. On Higher Order Systems

The authors note that the multiplicity study conducted here was only concerned about the presence of binary systems within the M-Dwarf population. No considerations were made to account for the presence of higher order (triple, quadruple, etc.) systems. While such systems do exist, they are relatively rare. A recent M-Dwarf multiplicity study found that only 3.3% of M-Dwarfs exist as triple and higher order systems (Winters et. al. (2019)). While the scope of this study is narrowed by excluding high order multiples, the conclusions regarding the binarity M-Dwarfs still hold because of the rarity of these higher order systems.

4.4. On the Interdependence of Mass Ratio and Orbital Separation

While this work is based on the view that the mass ratio of a stellar binary system does not depend on the separation between its components (as claimed by Reggiani Meyer (2013)), this is not a universally-held stance. Moe and Di Stefano (2017) definitively states that the distributions of mass ratio and period (which is directly proportional to separation) of systems with O- and B-type main sequence primaries are not independent. However, unlike Reggiani Meyer (2013), this conclusion was not reached considering M-dwarf primary systems. Further work exploring the interdependence of mass ratio and orbital separation for specifically type M stars will aid in making a conclusion.

4.5. Summary

We find that the distribution of M-Dwarf binary separations peaks at around 40 AU. Using this as well as other literature sources, we find that the multiplicity fraction over [0.60 ≤ q ≤ 1.00] and [0.00 ≤ a ≤ 10,000 AU] for M, FGK, and A stars to be 0.239 ± 0.04, 0.230 ± 0.032, and 0.238 ± 0.026 respectively. We note that these three values are all within error of one-another, suggesting that the multiplicity fraction does not vary strongly with spectral type. Future studies may explore the multiplicity fraction of OB-type stars and Brown Dwarfs to see if this trend holds with the most massive stars and smaller sub-stellar objects.

Acknowledgements. We thank the Formation and Evolution of Planetary Systems group for their consistent support. We also thank Dr. Max Moe and Dr. Kimberly Ward Duong for their insightful advice.

References

Bowler et. al. 2015, The Astrophys. Journal, 216, 1, 7
Cortes Contreras et. al. 2016 , Astro. & Astrophys., FC23
De Rosa et. al. 2013, Mon. Not. R. Astro. Soc. 437, 1216 1240
Delfosse et. al. 1998, Astro. & Astrophys., 344, 897 910
Fischer and Marcy 1992, The Astrophys. Journal, 396, 178 194
Janson et. al. 2012, The Astrophys. Journal, 754, 44 70
Moe and Di Stefano 2017, The Astrophys. Journal Supp. Series, 230:15
Raghavan et. al. 2010, The Astrophys. Journal, 190, 1 42
Reggiani and Meyer 2013, Astro. & Astrophys., 553, A124
Ward Duong et. al. 2015, Mon. Not. R. Astro. Soc. 000, 1 34
Winters et. al. 2019, In Press